

Supporting information for

Simultaneously enhancing the solubility and permeability of acyclovir by crystal engineering approach†

Yan Yan, Jia-Mei Chen*, and Tong-Bu Lu*

Experimental section

General remarks: Acyclovir was purchased from Wuhan Yuancheng Gongchuang Technology Co. Ltd. Maleic acid, fumaric acid and glutaric acid were purchased from Aladdin reagent Inc. All of the other chemicals and solvents were commercially available and used as received. Elemental analyses were determined using Elementar Vario EL elemental analyzer. Differential scanning calorimetry (DSC) was recorded on a Netzsch DSC-204 instrument and aluminium sample pans in nitrogen atmosphere, with a heating rate of 10 °C/min. The powder X-ray diffraction measurements were performed on D2 PHASER X-Ray Diffractometer. The single crystal data were collected on an Agilent Technologies Gemini A Ultra system.

Acyclovir/ maleic acid salt (1:1), 1: ACV·2/3H₂O (60 mg) was added to a nearly saturated solution of maleic acid (200 mg) in methanol (1 mL) and allowed to stir for 1 day at room temperature. The suspension was filtered and the isolated solid was dried under vacuum for 24 h at room temperature. Yield: 85.3 %. Elemental analysis:

calcd (%) for (C₁₂H₁₄N₅O₇ (**1**): C 44.17, H 4.33, N 17.17; found: C 44.20, H 4.57, N 17.37.

Acyclovir/fumaric acid cocrystal (1:1.5), 2: ACV·2/3H₂O (50 mg) was added to a nearly saturated solution of fumaric acid (100 mg) in methanol (1 mL) and allowed to stir for 5 days at room temperature. The suspension was filtered and the isolated solid was dried under a vacuum for 24 h at room temperature. Yield: 88.7 %. Elemental analysis: calcd (%) for C₁₄H₂₁N₅O₁₁(**2**): C 38.62, H 4.862, N 16.09; found: C 38.42, H 4.709, N 15.99.

Acyclovir/glutaric acid cocrystal (1:1), 3: ACV·2/3H₂O (50 mg) was added to a nearly saturated solution of glutaric acid (500 mg) in methanol (1 mL) and allowed to stir for 3 days at room temperature. The suspension was filtered and the isolated solid was dried under a vacuum for 24 h at room temperature. Yield: 84.6 %. Elemental analysis: calcd (%) for C₁₃H₁₉N₅O₇ (**3**): C 43.69, H 5.36, N 19.59; found: C 43.53, H 5.43, N 19.34.

Physical mixture of acyclovir with malic acid (1:1), 1-PM: ACV·2/3H₂O (100 mg) and maleic acid (48.9 mg) were milled to powder, and sieved using standard mesh sieves to provide powder samples with approximate particle size ranges of 75-150 μm, respectively. The two powders were mixed by a vortex mixer for 5 min at a shaking speed of 2500 rpm.

Physical mixture of acyclovir with fumaric acid (1:1.5), 2-PM: ACV·2/3H₂O (100 mg) and fumaric acid (73.4 mg) were milled to powder and sieved using

standard mesh sieves to provide powder samples with approximate particle size ranges of 75-150 μm , respectively. The two powders were mixed by a vortex mixer for 5 min at a shaking speed of 2500 rpm.

Physical mixture of acyclovir with glutaric acid (1:1), 3-PM: ACV·2/3H₂O (100 mg) and glutaric acid (55.7 mg) were milled to powder and sieved using standard mesh sieves to provide powder samples with approximate particle size ranges of 75-150 μm , respectively. The two powders were mixed by a vortex mixer for 5 min at a shaking speed of 2500 rpm.

Single crystal X-ray diffraction: Single-crystal X-ray diffraction data for **1-3** were collected on an Agilent Technologies Gemini A Ultra system with graphite monochromated Cu K α radiation ($\lambda = 1.54178 \text{ \AA}$). Cell refinement and data reduction were applied using the program of CrysAlis PRO.¹ The structures were solved by the direct methods using the SHELX-97 program,² and refined by the full-matrix least-squares method on F^2 . All non-hydrogen atoms were refined with anisotropic displacement parameters. Hydrogen positions on nitrogen and oxygen were located in Fourier-difference electron density maps. Hydrogen atoms associated with carbon atoms were refined in geometrically constrained riding positions.

Powder dissolution experiments: The absorbance values for ACV·2/3H₂O and **1-3** in phosphate buffer of pH 6.8 at different times were detected by a Cary 50 UV/vis spectrophotometry at 254 nm, where all the co-formers do not absorb at 254 nm. For experiment involving ACV·2/3H₂O and **1-3**, absorbance values were related

to solution concentrations using a calibration curve for acyclovir. All the solids were milled to powder and sieved using standard mesh sieves to provide samples with approximate particle size ranges of 75-150 μm . In a typical experiment, a flask containing 600 mg of sample was added 50 mL of phosphate buffer (pH 6.8), and the resulting suspension was stirred at 37 °C and 500 rpm. Aliquots were filtered through a 0.22 μm nylon filter after 5, 10, 15, 20, 30, 40, 50, 60, 90, 120, 150, 210, 270, 330 and 480 min. A 0.01 mL portion of the filtered aliquot was diluted to 1.0 mL with water and was measured with UV/vis-spectrophotometry. After the powder dissolution experiments (8 hours later), the undissolved solids were filtered and dried under vacuum, and analyzed by XRPD.

***In vitro* skin permeation experiments:** Three replicated experiments using Franz-type diffusion cells were carried out to compare the *in vitro* release of ACV·2/3H₂O, and **1-3** from polyethylene glycol 400 (PEG 400) ointment. Approximately 5 mg of acyclovir was mixed with 1 mL PEG 400 to form the ointment. The skin samples were excised from Sprague Dawley rats, 180-200 g. 7 mL of release medium (phosphate buffer of pH 6.8) was placed in the receptor chamber which was continuously stirred at 37 °C and 500 rpm. 0.3 mL aliquots of the release medium were withdrawn from the receptor chamber at predetermined times and replaced with the same volume of fresh phosphate buffer of pH 6.8. The release experiments lasted for 24 hours, and the concentrations of acyclovir and co-formers were determined by HPLC to calculate the cumulative amount of released acyclovir and co-formers.

High performance liquid chromatography analysis: HPLC analysis of acyclovir and cofomers was performed on a Shimadzu 20A HPLC system which equipped with Inertsil ODS-3 (150 × 4.6 mm I. D., 5 μm) column. The flow rate was 0.8 mL·min⁻¹ and the column temperature was ambient temperature. The mobile phase of ACV, **1** and **3** was consisted of phosphate buffer (pH = 2.4)/methanol (90:10), while the mobile phase of **2** was consisted of phosphate buffer (pH = 2.4)/methanol (95:5). UV analysis of ACV, maleic acid, fumaric acid and glutaric acid was detected at 254, 214, 214 and 204 nm, respectively.

Table 1. The hydrogen bonding distances and angles for **1-3**

D-H...A	D...A (Å)	D-H...A (deg)
1^a		
O9-H9...O8	2.431(2)	174.6
O3-H3...O10#1	2.932(3)	158.4
N1-H1N...O12	2.809(3)	168(3)
N2-H2B...O11	2.989(3)	175(3)
N2-H2A...N8#2	3.046(3)	171(3)
N5 ⁺ -H4N...O7 ⁻	2.682(3)	173(3)
O6-H6A...O3#3	2.785(3)	148.6
O6-H6A...O4#4	2.983(3)	127.6
N7-H7A...O9	2.997(3)	177(3)
N6-H2N...O10	2.770(3)	169(3)
N7-H7B...N3#5	3.169(3)	172(3)
N10 ⁺ -H9N...O14 ⁻ #6	2.642(3)	174(3)
O11-H11...O13	2.427(2)	176.0
2^b		
O1W-H1B...O9#1	2.762(3)	149.6

O1W-H1C...O9#2	2.768(3)	160.6
O2W-H2C...O5	2.705(3)	153.6
O2W-H2D...O1W	2.685(3)	158.7
N1-H1...O5	2.914(3)	158.8
N2-H2A...N3#3	3.113(3)	174.2
N2-H2B...O2W	2.969(3)	177.7
O3-H3...O2#1	2.659(2)	177.7
O6-H6A...O7	2.561(2)	175.5
O9-H9A...O2W#3	2.722(3)	173.7
O1-H1A...N5	2.567(3)	177.2
3^c		
O1-H1O...N5	2.663(19)	177(2)
O4-H4O...O5#1	2.541(18)	173(3)
N2-H2N...O3#2	2.998(2)	145(2)
N1-H1N...O3#3	2.943(19)	154.0(18)
N2-H3N...N3#4	3.054(2)	170.5(19)
O5-H5O...O7#5	2.638(18)	176(3)

Symmetry codes: ^a#1 x, y+1, z; #2 -x+1, -y+1, -z+1; #3 -x+2, -y, -z+2; #4 -x+2, -y-1, -z+2; #5 -x+1, -y+1, -z+1; #6 x+2, y-2, z+1; ^b#1 x, -y+1, z+1/2; #2 -x, y+1, -z+1/2; #3 -x, y, -z+1/2; #4 -x+1, y, -z+1/2; ^c#1 x, y-1, z-1; #2 x+1, y, z+1; #3 x+1, y, z+1; #4 -x+1, -y+2, -z+3; #5 x-1, y+1, z

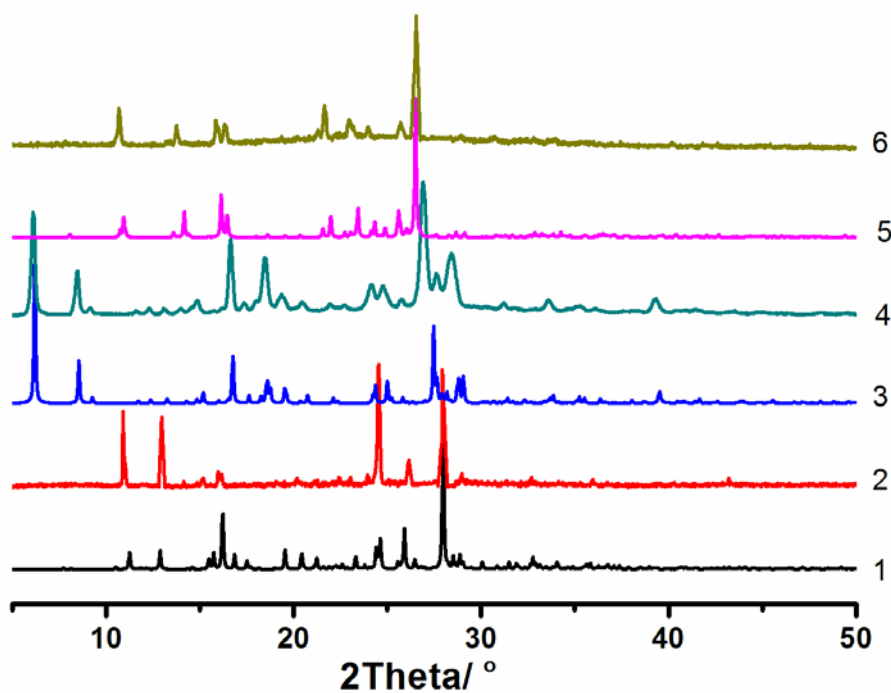


Fig S1. The simulated PXRD patterns generated from single-crystal diffraction data (1, 3, 5) and the measured PXRD patterns at room temperature (2, 4, 6) for **1** (1,2), **2** (3,4) and **3** (5,6), respectively.

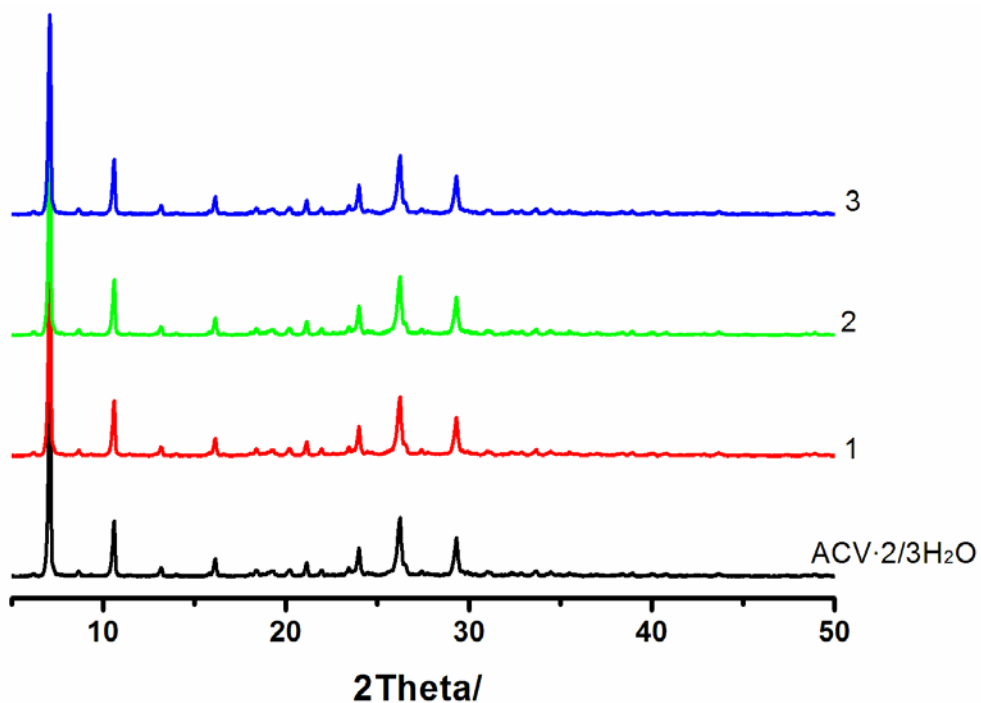


Fig S2. XRPD patterns after powder dissolution experiments in phosphate buffer of pH 6.8, indicating all the complexes converted to $\text{ACV} \cdot 2/3\text{H}_2\text{O}$.

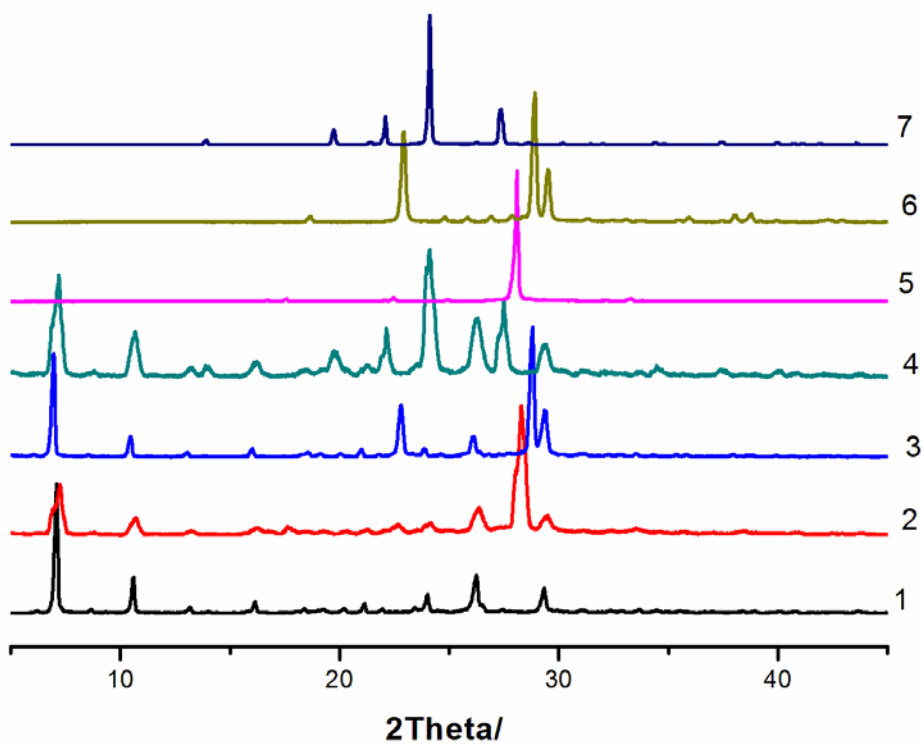


Fig S3. The PXR D patterns for ACV·2/3H₂O (1), 1-PM (2), 2-PM (3), 3-PM (4), maleic acid (5), fumaric acid (6) and glutaric acid (7), respectively.

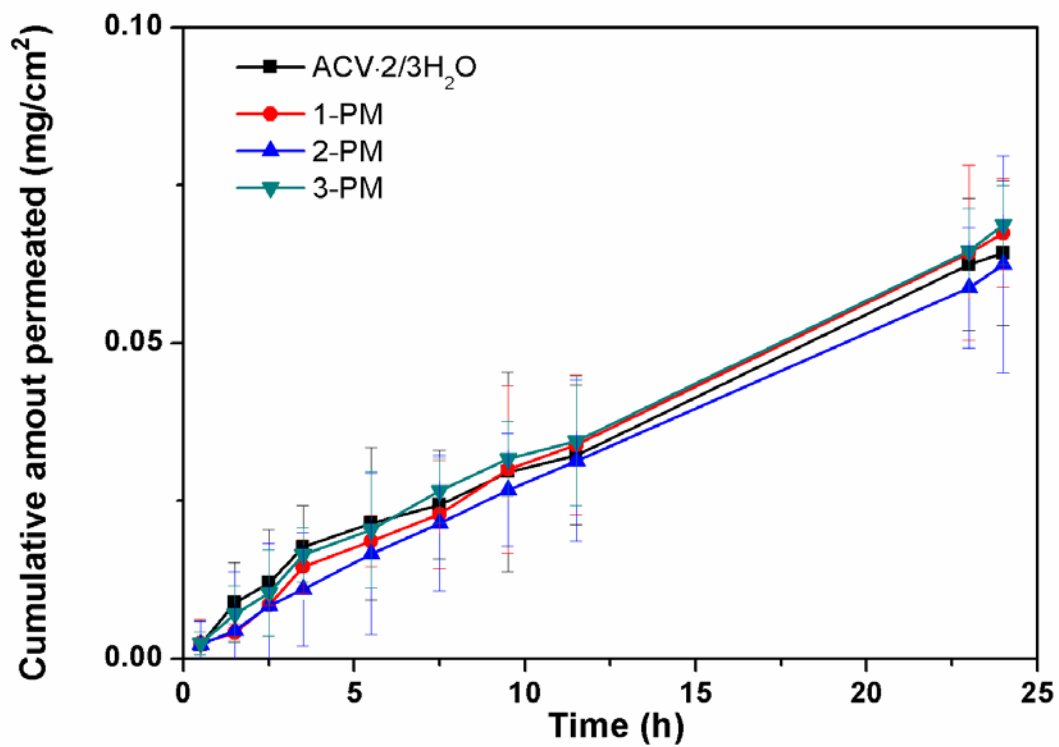
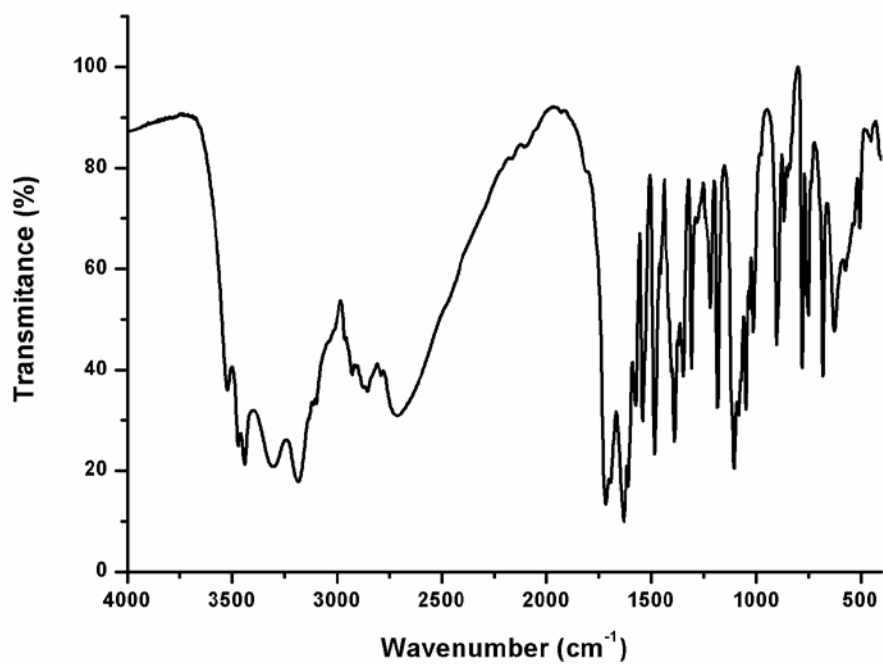
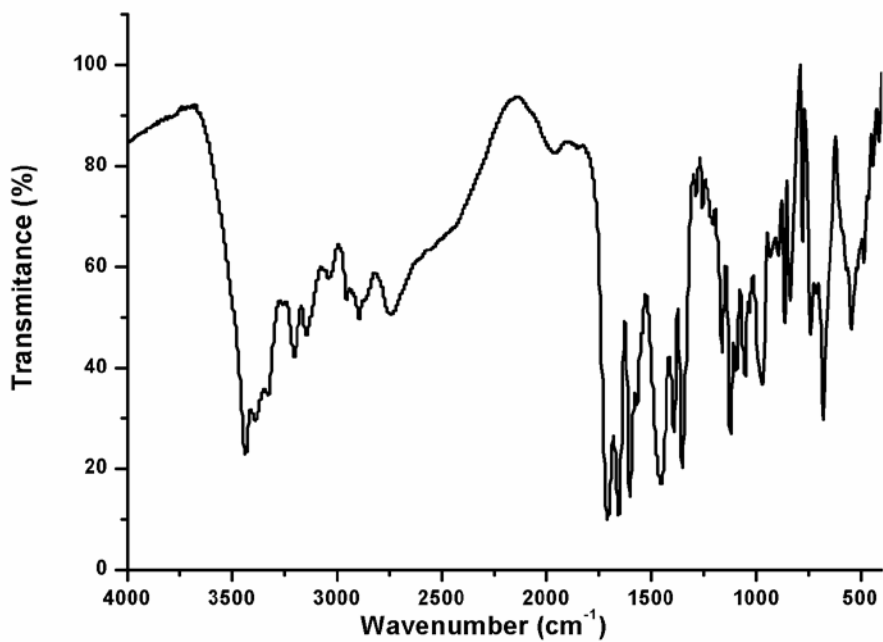


Fig S4. The permeation profiles of physical mixture of acyclovir and CCFs.

(a)



(b)



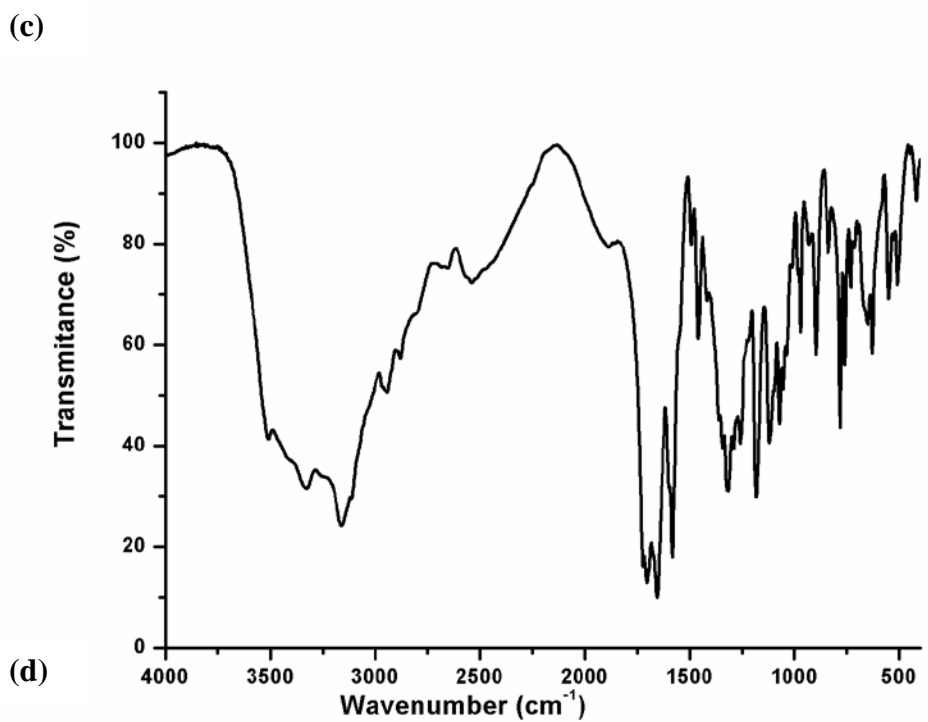


Fig S5. IR spectra for ACV·2/3H₂O (a), **1** (b), **2** (c) and **3** (d), respectively.

Reference

1. *CrysAlis^{Pro} Version 1.171.35.19.*, 2011, Agilent Technologies Inc., Santa Clara, CA, USA.
2. G. M. Sheldrick, *SHELXS 97, Program for Crystal Structure Refinement*; University of Göttingen, Göttingen, 1997.